

04,03

## Early formation of surface states in MOS structures under ionizing irradiation

© O.V. Alexandrov

St. Petersburg State Electrotechnical University „LETI“,  
St. Petersburg, Russia

E-mail: Aleksandr\_ov@mail.ru

Received February 22, 2023

Revised February 22, 2023

Accepted March 1, 2023

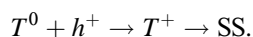
A quantitative model of the early formation of surface states (SS) in MOS structures under ionizing irradiation (II) with a limiting stage — dispersion transport of holes has been developed. According to the model, the main contribution to the early formation of SS occurs during the microsecond pulse II for a thin gate dielectric and after the end of the pulse for a thick field oxide. The increase in the density of early SS after the end of II is associated with the presence of localized states and the dispersion transport of holes. The late formation of SS is limited by the dispersion transport of hydrogen ions, which delays the formation of late SS from 0.1 to  $10^4$  seconds or more.

**Keywords:** MOSFET structure, ionizing irradiation, surface conditions, dispersion transport.

DOI: 10.21883/PSS.2023.05.56043.22

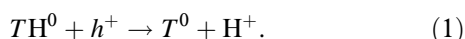
### 1. Introduction

It is commonly believed that there are two surface state (SS) formation mechanisms in MOS structures exposed to ionizing irradiation (II): conversion and hydrogen [1,2]. For the first mechanism, SS are formed by trapping II-generated  $h^+$  holes by hole traps  $T$  near Si–SiO<sub>2</sub> phase boundary (PB) followed by hole transformation (conversion) to SS:

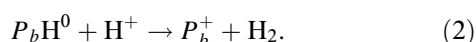


The transformation mechanism is still unclear [1]. It is suggested in [3] that transformation of the trapped  $T^+$  holes in SS occurs when an electron is trapped from the conduction band or when a hole is emitted into the valence band of a silicon substrate. In [4], instead of transformation, „border traps“ are introduced which are located in oxide at a distance less than 3 nm from PB and may exchange their charges with the silicon substrate enough quickly by tunneling mechanism, which makes them similar to SS.

By the hydrogen mechanism, SS are formed in a two-stage process [5]. At the first stage,  $H^+$  are released when holes are trapped by hydrogen-containing traps  $TH^0$ :



At the second stage, hydrogen ions drift to Si–SiO<sub>2</sub> PB where they depassivate  $P_bH$ -centers with SS formation ( $P_bH$ -centers):



It has been found that there are earlier formation of SS — within microseconds after II pulse [6–8] and later formation of SS that starts from 0.1–1 s and extends

to  $10^4$ – $10^5$  s [5–8]. Later formation of SS is well described by the hydrogen mechanism with a limiting stage — hydrogen transport [5–8]. Early formation of SS was associated with the conversion mechanism and limiting stage — hole transport [6–8]. An SS fraction formed by this mechanism accounts for 10–20% of the total density of SS formed after II [1,2].

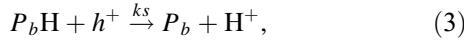
Hole and hydrogen transport in amorphous SiO<sub>2</sub> is dispersive in nature and is described by a continuous time random walk (CTRW) model [9–11], or multiple trapping model [12]. The multiple trapping model was used to perform quantitative description of SS formation by the hydrogen mechanism [13], II intensity impact [14] and latent SS accumulation [15]. Accumulation of space charge associated with dispersive transport of hole polarons at low (80–293 K) temperatures was addressed in [16]. Quantitative description of the early SS formation due to hole transport and trapping at standard temperatures is of interest.

The purpose of this study is to develop a quantitative model of early SS formation with ionizing irradiation of MOS structures.

### 2. Model description

Time of hole transport through thin gate SiO<sub>2</sub> of MOS structure will be assessed. With oxide thickness of  $d = 100$  nm and hole drift transport mechanism in  $E = 1 \cdot 10^6$  V/cm field with hole mobility  $\mu_p = 2 \cdot 10^{-5}$  cm<sup>2</sup>/V·s [17], this time is  $t = d/(\mu E) \cong 0.5 \mu\text{s}$  which approximately corresponded to early SS emergence. I.e. hole transport can be actually a limiting stage of early SS formation as was suggested in [6–8]. Conversion mechanism that is enabled when holes reach Si–SiO<sub>2</sub> PB is not the limiting stage in this case.

Earlier papers [18–20] suggested that hole trapping may result in rupture of weak bonds Si–H and Si–OH [18,19] or strained bonds Si–O [21] at Si–SiO<sub>2</sub> PB. During hole injection from the silicon substrate, formation of positive charge in oxide and of SS at Si–SiO<sub>2</sub> PB were observed [22,23]. It is supposed that early SS are formed by means of weak hydrogen bond rupture in  $P_b$ H-centers at Si–SiO<sub>2</sub> PB when  $h^+$  holes generated by II are trapped according to the following reaction

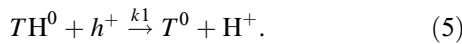


where  $k_s$  is the reaction rate constant. Hydrogen released in this reaction forms SS according to reaction (2). Early SS density  $Q_{ite}$  will be defined by the depassivation rate of  $P_b$ H-centers according to reaction (3)

$$\frac{\partial Q_{P_b}}{\partial t} = k_s Q_{P_b} H, \quad (4)$$

where  $t$  is time,  $Q_{P_bH}$  and  $Q_{P_b}$  are densities of passivated and unpassivated  $P_b$ -centers ( $Q_{ite} = Q_{P_b}$ ),  $p$  are concentrations of free holes at Si–SiO<sub>2</sub> PB.

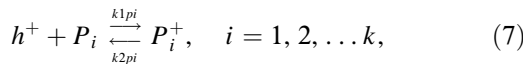
To calculate hole concentration variation kinetics during and after II, hole consumption in the reaction of hydrogen release from the hydrogen-containing trap



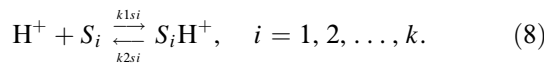
and hole trapping by hydrogen-free hole traps formed in reaction (5) shall be considered:



For this, dispersive nature of hole transport in amorphous SiO<sub>2</sub> with formation of hole polarons  $P_i^+$  and dispersive nature of hydrogen ion transport shall be considered. Dispersive hole transport will be described using the model of multiple trapping to localized  $P_i$  states [16]:



where  $k$  is the number of localized states. Dispersive hydrogen ion transport will be described using the model of multiple trapping to localized  $S_i$  states [13]:



Hole and hydrogen ion transport equations together with Poisson equation are written as

$$\begin{aligned} \frac{\partial p}{\partial t} = & D_p \frac{\partial^2 p}{\partial x^2} - \mu_p \frac{\partial(Ep)}{\partial x} - (k_2 C_T^0 + k_1 C_{TH}^0) p \\ & - \sum_{i=1}^k k_{1pi} C_{Pi}^0 p + \sum_{i=1}^k k_{2pi} C_{Pi}^+ + G, \end{aligned} \quad (9)$$

$$\begin{aligned} \frac{\partial C_H^+}{\partial t} = & D_H^+ \frac{\partial^2 C_H^+}{\partial x^2} - \mu_H^+ \frac{\partial EC_H^+}{\partial x} + k_1 C_{TH}^0 p \\ & - C_H^+ \sum_{i=1}^k k_{1si} C_{Si}^0 + \sum_{i=1}^k k_{2si} C_{SHi}^+, \end{aligned} \quad (10)$$

$$\frac{\partial^2 V}{\partial x^2} = -\frac{q}{\epsilon \epsilon_0} \left( p + C_T^+ + C_H^+ + \sum_{i=1}^k (C_{Pi}^+ + C_{SHi}^+) \right), \quad (11)$$

where  $x$  is the coordinate counted from silicon substrate PB with  $x = 0$  to gate PB with  $x = d$ ,  $d$  is the dielectric thickness;  $C_T^0$  and  $C_{TH}^0$  is the concentrations of neutral hydrogen-free and hydrogen-containing hole traps,  $C_T^+$  and  $C_H^+$  is the concentration of positively charged traps and free hydrogen ions,  $C_{Pi}^0$  and  $C_{Pi}^+$  are concentrations of  $i$ -th empty and filled polaron states, respectively;  $C_{Si}^0$  and  $C_{SHi}^+$  are concentrations of  $i$ -th empty and filled hydrogen states, respectively;  $D_p$  and  $\mu_p$  are the diffusion coefficient and hole mobility, respectively ( $\mu_p = 2 \cdot 10^{-5} \text{ cm}^2/\text{V} \cdot \text{s}$  [17],  $D_p = k_B T \mu_p$ ,  $k_B$  is the Boltzmann constant,  $T$  is the temperature,  $T = 300 \text{ K}$ );  $D_H^+$  and  $\mu_H^+$  are diffusion coefficient and free hydrogen ion mobility, respectively ( $D_H^+ = 1 \exp(-0.73/(k_B T)) \text{ cm}^2/\text{s}$  [24],  $\mu_H^+ = D_H^+/(k_B T)$ );  $V$  is the potential,  $E$  is the electric field strength,  $E = -dV/dx$ ,  $q$  is the electron charge;  $\epsilon$  is the relative dielectric constant of silicon oxide ( $\epsilon = 3.9$ ),  $\epsilon_0$  is the Coulomb constant. Rate of electron-hole pair generation  $G$  is determined by irradiation dose rate  $F$ , coefficient of electron-hole pair generation  $k_g$  and probability of pair separation by an electric field  $f_y(E)$ :  $G(E) = F k_g f_y(E)$ , where  $k_g(\text{SiO}_2) = 8.1 \cdot 10^{12} \text{ cm}^{-3}/\text{rad}$ . The following approximation was used for  $f_y(E)$  [25]:

$$f_y(E) = \left[ \frac{0.27}{(E + 0.084)} + 1 \right]^{-1},$$

where  $E$  is in MV/cm.

Equations (9)–(11) are solved together with the kinetic equations for immobile reaction components.

Distribution of localized state density for holes is exponential by energy which is specific to noncrystalline materials [26], and by coordinate

$$C_{Pi}^0(E_{Pi}) = N_p^0 \exp\left(-\frac{E_{Pi}}{E_{PP}}\right) \exp\left(-\frac{x}{L_P}\right), \quad i = 1, 2, \dots, k, \quad (12)$$

where  $N_p^0$  is total polar concentration of empty and filled hole polaron states,  $N_p^0 = C_p^0 + C_p^+$ ,  $C_p^0 = \sum_{i=1}^k C_{Pi}^0$ ,

$C_p^+ = \sum_{i=1}^k C_{Pi}^+$ ;  $E_{Pi}$  is the  $i$ -th polaron state level energy,  $E_{PP}$  is the characteristic polaron energy related to dispersive hole parameter  $\alpha_p$  by  $\alpha_p = k_B T/E_{PP}$ ,  $L_P$  is the distribution width ( $L_P = 10 \text{ nm}$  was assumed).

Localized state density distribution for hydrogen ions is exponential by energy and uniform by coordinate

$$C_{Si}^0(E_{Si}) = N_S^0 \exp\left(-\frac{E_{Si}}{E_{SS}}\right), \quad i = 1, 2, \dots, k, \quad (13)$$

where  $N_S^0$  is the total concentration of empty and filled hydrogen states,  $N_S^0 = C_S^0 + C_{SH}^+$ ,  $C_S^0 = \sum_{i=1}^k C_{Si}^0$ ,  $C_{SH}^+ = \sum_{i=1}^k C_{SHi}^+$ ;  $E_{Si}$  is the  $i$ -th polaron state level energy;  $E_{SS}$  is the characteristic energy related to dispersive hydrogen parameter  $\alpha_S$  by  $\alpha_S = k_B T / E_{SS}$ .

In the initial point of time, concentrations of holes, hydrogen ions and their filled states are equal to zero

$$p(x, 0) = 0, \quad C_H^+(x, 0) = 0, \quad C_{Pi}^+(x, 0) = 0, \\ C_{Si}^+(x, 0) = 0, \quad i = 1, 2, \dots, k. \quad (14)$$

Concentration of neutral hydrogen-containing traps was assumed uniform in depth

$$C_{TH}^0(x, 0) = C_{TH0}^0. \quad (15)$$

Boundary condition for free holes at  $x = 0$  depends on the hole flow rate to Si–SiO<sub>2</sub> PB according to (4):

$$j_p = \frac{\partial Q_{Pb}}{\partial t}, \quad (16)$$

where  $j_p$  is the hole flow,  $j_p = -D_p \frac{\partial p}{\partial x} + \mu_p p E$ . With  $x = d$ , an absorbing boundary for holes like a gate for free hydrogen ions at both Si–SiO<sub>2</sub> and SiO<sub>2</sub> PB are assumed

$$p(d, t) = C_H^+(0, t) = C_H^+(d, t) = 0. \quad (17)$$

$V_G$  voltage is applied to the gate at  $x = d$ :

$$V(0, t) = 0, \quad V(d, t) = V_G. \quad (18)$$

Formation of late SS occurs after H<sup>+</sup> release from the hydrogen-containing trap by reaction (5) and following depassivation of  $P_b$ H-centers by reaction (2). Thus, density of late SS  $Q_{itl}$  is defined by integral hydrogen ion flow  $j_H^+$  at PB:

$$Q_{itl} = \int_0^t j_H^+(0, t) dt. \quad (19)$$

Fitting of the following parameters was carried out for calculation: concentration of neutral hydrogen-containing traps  $C_{TH0}^0$  and reaction rate constant  $k_S$  (3). For other parameters, previously determined values were taken for hole transport in [16]:  $N_p^0 = 2.2 \cdot 10^{19} \text{ cm}^{-3}$ ,  $E_{p1} = 0.26 \text{ eV}$ ,  $E_{pk} = 0.55 \text{ eV}$ ,  $E_{pp} = 0.2 \text{ eV}$  (with  $T = 300 \text{ K}$ ,  $E = 1 \text{ MV/cm}$ ) and for hydrogen ion transport in [13,14]:  $N_S^0 = 6 \cdot 10^{22} \text{ cm}^{-3}$ ,  $E_{S1} = 0.65 \text{ eV}$ ,  $E_{Sk} = 0.98 \text{ eV}$ ,  $E_{SS} = 0.07 \text{ eV}$ .

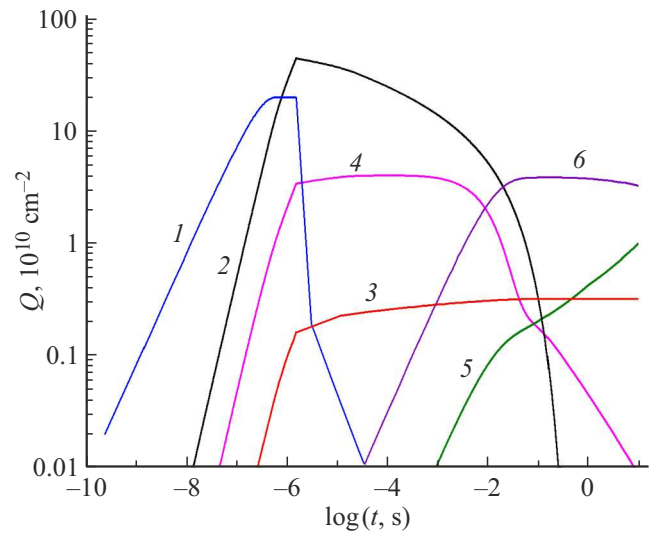


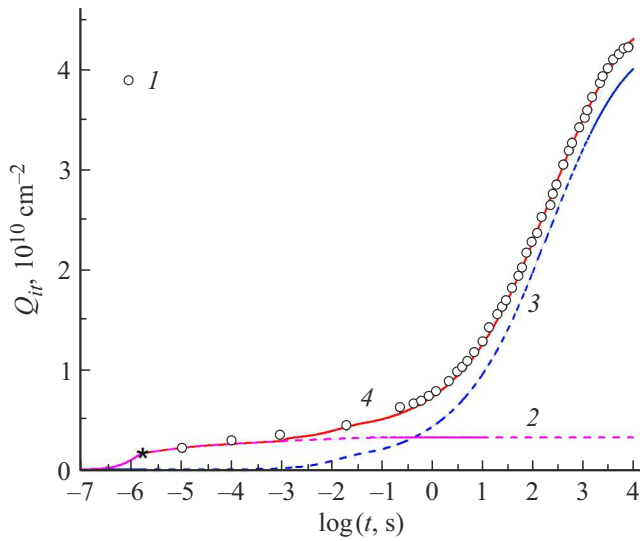
**Figure 1.** Time dependences  $Q_P$  (1),  $Q_P^+$  (2),  $Q_{ite}$  (3),  $Q_H^+$  (4),  $Q_{itl}$  (5) and  $Q_{SH}^+$  (6). (Calculation parameters as for Figure 2).

### 3. Calculation results

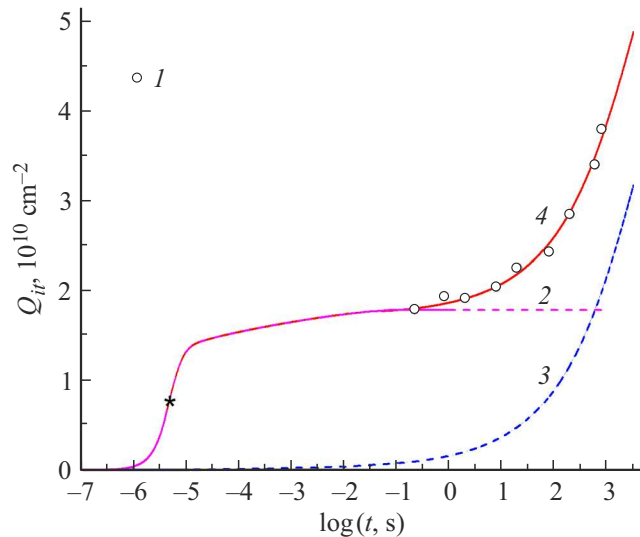
Equations (9)–(11) were solved numerically by implicit difference scheme with initial conditions (12)–(15) and boundary conditions (16)–(18). Density of early SS was calculated using (4), late SS were calculated using (19).

Figure 1 shows time dependences of integral concentrations of free holes  $Q_P = \int_0^d p dx$  (curve 1), holes trapped to localized hole states  $Q_P^+ = \int_0^d C_P^+ dx$  (curve 2), and of free hydrogen ions  $Q_H^+ = \int_0^d C_H^+ dx$  (curve 4) and hydrogen ions trapped to localized hydrogen states  $Q_{SH}^+ = \int_0^d C_{SH}^+ dx$  (curve 6).

As shown in Figure 1, during II pulse (curve 1), the number of free holes  $Q_P$  grows up to saturation at  $t \sim 0.3 \mu\text{s}$ , and the number of holes trapped to the localized states  $Q_P^+$  grows (curve 2). After pulse end, the number of free holes (curve 1), first, drops dramatically due to the hole generation stop, and then drop more gradually due to the hole flow to PB. The number of holes accumulated on localized states (curve 2) decreases much slower after pulse end than the number of free holes, and contributes to the growth of early SS. Density of early SS  $Q_{ite}$  (curve 3) grows quickly during the pulse and more slowly after pulse end up to saturation at  $\sim 0.1 \text{ s}$ . The number of free hydrogen ions  $Q_H^+$  (curve 4) grows quickly during II, and is almost unchanged after II up to  $\sim 1 \text{ ms}$ , and then drops due to H<sup>+</sup> flow to PB and, thus, provides the growth of late SS  $Q_{itl}$  (curve 5). The amount of hydrogen accumulated on localized states  $Q_{SH}^+$  (curve 6) first grows after pulse end, then gradually drops beginning from  $\sim 0.1 \text{ s}$ , contributing to the growth of late SS.



**Figure 2.** Time dependences of SS density: 1 — experiment [8], 2–4 — calculation: 2 —  $Q_{ite}$ , 3 —  $Q_{itl}$ , 4 —  $Q_{it}$  ( $d = 42$  nm,  $C_{TH0}^0 = 3.2 \cdot 10^{18}$  cm $^{-2}$ ,  $k_s = 6 \cdot 10^{-15}$  cm $^3$ /s).



**Figure 3.** Time dependences of SS density: 1 — experiment [27], 2–4 — calculation: 2 —  $Q_{ite}$ , 3 —  $Q_{itl}$ , 4 —  $Q_{it}$  ( $d = 800$  nm,  $C_{TH0}^0 = 4.7 \cdot 10^{17}$  cm $^{-2}$ ,  $k_s = 2 \cdot 10^{-14}$  cm $^3$ /s).

The calculations were compared with the experimental data [8] on irradiation of MOS structures with thin gate oxide ( $d = 42$  nm) by 40 MeV electron pulse with equivalent dose 46.6 krad and duration 1.5  $\mu$ s. Voltage  $V_G = +4.2$  V was applied to the gate ( $E = 1$  MV/cm). Figure 2 shows experimental data [8] (symbols 1) and calculated dependences of early  $Q_{ite}$  (curve 2), late  $Q_{itl}$  (curve 3) and total  $Q_{it} = Q_{ite} + Q_{itl}$  (curve 4) SS density during and after 1.5  $\mu$ s pulse end (symbol \* on dependence  $Q_{ite}(t)$ ).

The calculations were also compared with the experimental data [27] on irradiation of MOS structures with thick field oxide ( $d = 800$  nm) by 40 MeV electron pulse with equivalent dose 10 krad and duration 4  $\mu$ s. Voltage

$V_G = +160$  V was applied to the gate ( $E = 2$  MV/cm). In [27], energy density of SS  $D_{it}$  was determined at the surface potential maximum. Integral SS density is supposed as  $Q_{it} \cong 0.1D_{it}E_G$ , where  $E_G$  is the silicon band gap.

Figure 3 shows experimental data [27] (symbols 1) and calculated dependences of early  $Q_{ite}$  (curve 2), late  $Q_{itl}$  (curve 3) and total  $Q_{it} = Q_{ite} + Q_{itl}$  (curve 4) SS density during and after 4  $\mu$ s pulse end (symbol \* on dependence  $Q_{ite}(t)$ ).

The number of early SS  $Q_{ite}$  is defined by the number of free holes formed during II, hole trap cross-section in the reaction rate constant (3), and also by the number of holes accumulated on localized hole states  $Q_P^+$ . The number of late SS  $Q_{itl}$  is defined by the number of free hydrogen ions released during II by reaction (5) and flown to Si–SiO $_2$  PB, and by the amount of hydrogen accumulated on localized hydrogen states  $Q_H^+$ .

It should be noted that in case of thick oxide, a significant fraction of early SS is formed after the pulse end, which is associated with longer dispersive hole transport from within the oxide to the silicon substrate PB. Holes accumulated on the localized hole states delay the attainment of saturation by  $Q_{ite}(t)$ . In the similar way, hydrogen accumulated on the localized hydrogen states delays the growth of  $Q_{itl}(t)$ .

It should be noted that the early SS formation rate constant for thick field oxide is  $\sim 3$  times higher than for thin gate oxide. This is explained by higher electrical field strength and, thus, by higher hole energy in reaction (3) for the field oxide. Assuming that the early SS formation rate constant is defined by the hole drift rate,  $k_s = \sigma_p \mu_p E$ , the following enters are derived for the hole trap cross-section on  $P_bH$ -centers:  $\sigma_p = 3 \cdot 10^{-14}$  cm $^2$  for thin gate oxide and  $\sigma_p = 5 \cdot 10^{-14}$  cm $^2$  for thick field oxide.

The number of hydrogen-containing hole traps both in gate and field oxides ( $Q_{TH0}^0 = C_{TH0}^0 d = 1.3 \cdot 10^{13}$  and  $3.8 \cdot 10^{13}$  cm $^{-2}$ , respectively) is rather high compared with the number of holes generated during II ( $Q_P = Gt = 1.3 \cdot 10^{12}$  and  $5.7 \cdot 10^{12}$  cm $^{-2}$ , respectively). Therefore, with rather long durations after II, the density of late SS becomes higher than the density of early SS both in thin gate and thick field oxides.

## 4. Conclusions

A quantitative model of early SS formation in MOS structures during II with limiting stage — dispersive hole transport — has been developed. According to this (hole) model, the main contribution to the early SS formation takes place during the microsecond II pulse for thin gate dielectric and after the pulse end for thick field oxide. Growth of early SS density after II end is associated with the presence of localized states and dispersive hole transport. Late SS formation is limited by dispersive hydrogen ion transport. The presence of localized hydrogen states delays the late SS formation from  $\sim 0.1$  s

to  $10^4$  and more seconds. SS density calculation agrees with the experiments [8,27] with other main parameters determined earlier for holes in [16] and for hydrogen ions in [13,14].

### Conflict of interest

The author has no conflict of interest.

### References

- [1] T.R. Oldham, F.B. McLean. IEEE Trans. Nucl. Sci. **50**, 3, 483 (2003).
- [2] K.I. Tapero, V.N. Ulimov, A.M. Chlenov. Radiatsionnye efekty v kremnievykh integral'nykh skhemakh kosmicheskogo primeneniya BINOM M. (2012). 304 p. (in Russian).
- [3] V.S. Pershenkov, D.V. Savchenko, A.S. Bakarenkov, V.N. Ulimov. Mikroelektronika, **39**, 2, 102 (2010). (in Russian).
- [4] D.M. Fleetwood. IEEE NS-**39**, 2, 269 (1992).
- [5] F.B. McLean. IEEE Trans. Nucl. Sci. **27**, 6, 1651 (1980).
- [6] J.R. Schwank, P.S. Winokur, F.W. Sexton, D.M. Fleetwood, J.H. Perry, P.V. Dressendorfer, D.T. Sanders, D.C. Turpin. IEEE Trans. Nucl. Sci. **33**, 6, 1178 (1986).
- [7] H.E. Boesch. IEEE Trans. Nucl. Sci. **35**, 6, 1160 (1988).
- [8] N.S. Saks, C.M. Dozier, D.B. Brown. IEEE Trans. Nucl. Sci. **35**, 6, 1168 (1988).
- [9] F.B. McLean, N.E. Boesch, J.M. McGarrity. IEEE Trans. Nucl. Sci. **23**, 6, 1506 (1976).
- [10] N.E. Boesch, J.M. McGarrity, F.B. McLean. IEEE Trans. Nucl. Sci. **25**, 3, 1012 (1978).
- [11] N.E. Boesch, F.B. McLean, J.M. McGarrity, P.S. Winokur. IEEE Trans. Nucl. Sci. **25**, 6, 1239 (1978).
- [12] O.L. Curtis, J.R. Srour. J. Appl. Phys., **48**, 9, 3819 (1977).
- [13] O.V. Aleksandrov. FTP **54**, 10, 1029 (2020). (in Russian).
- [14] O.V. Aleksandrov. FTP **55**, 2, 152 (2021). (in Russian).
- [15] O.V. Aleksandrov. FTP **55**, 2, 152 (2021). (in Russian).
- [16] O.V. Aleksandrov. FTP **56**, 12, 1154 (2022). (in Russian).
- [17] R.C. Hughes. Phys. Rev. **B15**, 4, 2012 (1977).
- [18] A.G. Revesz. J. Electrochem. Soc. **126**, 1, 122 (1979).
- [19] P.S. Winokur, H.E. Boesch, J.M. McGarrity, F.B. McLean. J. Appl. Phys. **50**, 5, 3492 (1979).
- [20] S.K. Lai. J. Appl. Phys. **54**, 5, 2540 (1983).
- [21] F.J. Grunthaner, P.J. Grunthaner. Mater. Sci. Rep. **1**, 65 (1986).
- [22] Q.D. Khosru, N. Yasuda, K. Taniguchi, C. Hamaguchi. Appl. Phys. Lett. **63**, 18, 2537 (1993).
- [23] G. Van den Bosch, G. Groeseneken, H.E. Maes, R.B. Klein, N.S. Saks. J. Appl. Phys. **75**, 4, 2073 (1994).
- [24] S.R. Hofstein. IEEE Trans. El. Dev. **14**, 11, 749 (1967).
- [25] J.M. Benedetto, H.E. Boesch. IEEE Trans. Nucl. Sci. **33**, 6, 1318 (1986).
- [26] V.I. Arkhipov, A.I. Rudenko. Phil. Mag. B **45**, 2, 189, 209 (1982).
- [27] N.E. Boesch, T.L. Taylor. IEEE Trans. Nucl. Sci. **31**, 6, 1273 (1984).

*Translated by E.Ilyinskaya*